

**X-ray photoelectron spectroscopy of GaP_{1-x}N_x photocorroded as a result of hydrogen
production through water electrolysis**

Marie A. Mayer

Office of Science, Science Undergraduate Laboratory Internship (SULI)

University of Illinois at Urbana-Champaign

Stanford Synchrotron Radiation Laboratory at the Stanford Linear Accelerator Center

Menlo Park, CA

August 18, 2006

Prepared in partial fulfillment of the requirements of the Office of Science, Department of Energy's Science Undergraduate Laboratory Internship under the direction of A. Nilsson in the Stanford Synchrotron Radiation Laboratory at Stanford Linear Accelerator Center.

Participant: _____

Signature

Research Advisor: _____

Signature

Table of Contents

Abstract	2
1. Introduction	3
2. Materials and Methods	5
3. Results	8
4. Discussion and Conclusions	9
5. Acknowledgements	10
6. References	11
8. Figures	13

ABSTRACT

X-ray photoelectron spectroscopy of $\text{GaP}_{1-x}\text{N}_x$ photocorroded as a result of hydrogen production through water electrolysis. MARIE A. MAYER (University of Illinois at Urbana-Champaign, Urbana, IL 61801) ANDERS NILSSON (Stanford Linear Accelerator Center, Menlo Park, CA, 94025).

Photoelectrochemical (PEC) cells produce hydrogen gas through the sunlight driven electrolysis of water. By extracting hydrogen and oxygen from water and storing solar energy in the H-H bond, they offer a promising renewable energy technology. Addition of dilute amounts of nitrogen to III-V semiconductors has been shown to dramatically increase the stability of these materials for hydrogen production. In an effort to learn more about the origin of semiconductor photocorrosion in PEC cells, three samples of p-type GaP with varying levels of nitrogen content (0%, 0.2%, 2%) were photocorroded and examined by X-ray Photoelectron Spectroscopy (XPS). GaPN samples were observed to be more efficient during the hydrogen production process than the pure GaP samples. Sample surfaces contained gallium oxides in the form of Ga_2O_3 and $\text{Ga}(\text{OH})_3$ and phosphorus oxide (P_2O_5), as well as surface oxides from exposure to air. A significant shift in intensity from bulk to surface peaks dramatic nitrogen segregation to the surface during photoelectrochemical hydrogen production. Further investigations, including using a scanning electron microscope to investigate sample topography and inductively coupled plasma mass spectroscopy (ICP-MS) analysis for solution analyses, are under way to determine the mechanism for these changes.

1. INTRODUCTION

1.1 Background

As fuel costs increase and supplies become increasingly limited, the demand for alternative energy sources rises. The fuel consumption of the United States in 2004 consisted of 94% fossil fuels, with only 1% of renewable energy originating from sunlight [1]. However, since the sun produces the equivalent of 1.3 trillion barrels of oil in a year; the remaining challenge is how to harvest this energy. [2] Photoelectrochemical (PEC) cells produce hydrogen gas through the sunlight driven electrolysis of water. By extracting hydrogen and oxygen from water and storing solar energy in the H-H bond, they offer a promising renewable energy technology. This technology has provided energy conversion efficiencies of up to 12.4% using multijunction regenerative solar cells [3], but suffers due to instability from photocorrosion.

A PEC cell has a typical electrochemical cell setup (Figure 1.1), with a p-type semiconductor cathode and a metal anode (or vice versa in the case of an n-type semiconductor). Both electrodes are immersed in electrolyte, which for hydrogen production would be water or a slightly acidic solution to increase the count of hydronium ions. The semiconductor-electrolyte interface forms the Helmholtz layer, which causes band bending. A further discussion of the physics of the semiconductors is given by Bak *et al.* [2]. When illuminated by sunlight, optically-excited holes diffuse to the bulk of the p-type semiconductor, while the minority carrier electrons travel to the semiconductor-electrolyte interface. The electrons reduce hydrogen contained in water molecules according to:



The holes travel through an electrical connection from the cathode to the anode, or oxidation site:

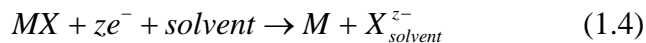


Since the gases are generated at different electrodes, they are easily separable. The H₂ is retained as fuel which, when used in a fuel cell to generate electricity, recombines with oxygen in the air to produce water and heat as the only byproducts, completing the pollution-free renewable energy cycle.

1.2 Materials Requirements

The reaction requires a band gap of approximately 2 eV: 1.23 eV required for completion of reactions 1.1 and 1.2, plus an additional voltage wasted on overpotentials [2]. The semiconductor chosen must also be conducive to absorbance of solar energy. A smaller band gap is ideal to absorb the maximum number of photons. Additionally, the valence band of the semiconductor must be more positive than that of the oxidation electropotential and the conduction band more negative than the reduction electropotential on an electrochemical scale (Figure 1.2). If a single-junction system is under consideration, few materials have a band gap that efficiently appeases both the electrolysis and efficient solar energy conditions.

There is also the issue of corrosion, or decomposition of the semiconductor, to consider. The greater the damage to the semiconductor surface, the less functional the cell. Oxidation (Equation 1.3) can dislodge metal ions from the semiconductor surface, while reduction (Equation 1.4) of the semiconductor can result in the formation of a thin layer of metal on the semiconductor surface.



Corrosion is dependent upon the thermodynamic and kinetic stability of the sample, which is, on a simple level, observable in terms of the values of corrosion potentials with respect to hydrolysis potentials. For corrosion to occur, the electropotentials associated with the corrosion

reactions would need to lie between the oxidation and reduction electropotentials for hydrolysis, as well as outside of the semiconductor band edges if the sample is under illumination (Figure 1.3). [4]

While there are a number of ways to address the band alignment and corrosion, alloying has produced positive effects on both accounts. In the GaP system, the effect of nitrogen on the band gap of these materials is twofold: nitrogen shifts the band gap transition toward direct alignment; and it shifts the band edges to a more favorable position compared to the water red-ox electropotentials. Nitrogen content up to approximately 2% has been shown to decrease corrosion, but at higher concentrations, the stability of the sample is threatened. The addition of nitrogen adds resistance to chemical attack, but the exact nature of the influence on photocorrosion is an open question. [5]

As an effort to learn more about the photocorrosion of p-type semiconductors in PEC hydrogen production, three samples of $\text{GaP}_x\text{N}_{1-x}$ (band gap of 2.25 eV [6]) with varying amounts of infused nitrogen ($x = 0, 0.002, 0.02$) were photocorroded and examined by synchrotron X-ray photoelectron spectroscopy (XPS). The objective included probing the surface before and after corrosion to learn about the causes of corrosion and effects of nitrogen. The possibilities of energy conversion with renewable resources depend upon the stability of the materials available.

2. MATERIALS AND METHODS

$\text{GaP}_{1-x}\text{N}_x$ ($x = 0, 0.02, 0.002$) samples were grown at the National Renewable Energy Laboratory (NREL) by metal-organic chemical vapor deposition (MOCVD). Samples were cleaved into two pieces; one piece was reserved as an uncorroded standard, while the remaining piece of each was photocorroded.

2.1 Electrochemical Corrosion

In order to accommodate acidic and vacuum environments, electrochemistry was performed using a mechanical cell made of Pyrex and Teflon (Figure 2.1). This cell exposed only the surface of the semiconductor to the solution, and the back contact was electrically connected to the potentiostat. The platinum counter electrode and Ag/AgCl reference electrodes were inserted as shown. Photocorrosion was done using a Gamry PHE200 potentiostat.

The Gamry chronopotentiometry program was used to record current vs. time and potential vs. time. The GaP_{1-x}N_x samples were etched with concentrated sulfuric acid, then immersed in a deaerated solution of 3M sulfuric acid, along with a Ag/AgCl reference electrode and a platinum counter electrode. An optical lamp was focused on the sample for the duration of corrosion. In order to evolve hydrogen under 100mW/cm² (1 sun) conditions, a cathodic current of 1.57 mA was passed through the sample for 8 hours, resulting in the charge passage of 45.2 C. Samples were stored in vacuum, disregarding transport times. The solution was retained for inductively coupled plasma mass spectroscopy (ICP-MS) analysis.

During hydrogen production, a qualitative examination revealed that the GaP_{0.98}N_{0.02} sample, which showed the most visible surface change, was the most effective at reducing the solution for the entire 8 hours. Bubbles from the GaP_{0.998}N_{0.002} sample appeared, but had decreased in number after 8 hours. GaP showed few obvious bubbles during hydrogen production, although there was a slight surface change.

2.2 XPS Measurements

Core level spectroscopy was used to study the surfaces of the corroded GaP_{1-x}N_x samples. X-ray photoelectron spectroscopy (XPS) was performed using synchrotron x-ray radiation at the Stanford Synchrotron Radiation Laboratory (SSRL) on beamline 5-2. The x-ray energy used set the kinetic energies of the released electrons according to:

$$E_{kin} = h\nu - E_B - \Phi \quad [7] \quad (2.1)$$

Here, $h\nu$ is the energy of the x-ray photon, E_B is the binding energy of the electron and Φ is the work function of the analyzed sample. Since the x-ray energy is tuneable and the work function is fixed, the binding energy reveals information about the surface structure: elements present and their nearest neighbors, as well as binding structures.

The structure of the corroded surface can change as a function of depth. A depth profile can be collected by measuring spectra at different photoelectron kinetic energies, due to the relationship between the mean free path of an electron and its kinetic energy, as shown in Figure 2.2. In synchrotron-based XPS, the kinetic energy of a photoelectron can be altered by changing the x-ray photon energy. Therefore, a given x-ray photon energy will emit an electron of a particular element with a specific mean free path.

$$\Delta = \lambda_i \cos(\alpha) \quad [8] \quad (2.2)$$

Equation 2.2 shows that the mean escape depth (Δ) is related to the mean free path (λ_i) through the emission angle of the electron. Therefore, by equation 2.2, the elements present at a specific depth can be monitored as a method to compare the oxide throughout the surface layers.

XPS was measured for six samples, as grown (at NREL by MOCVD) and a corroded sample of each GaP_{1-x}N_x ($x = 0, 0.002, 0.02$) In order to calibrate energies, gold deposited on Si was placed between the samples, and the Au 4f^{7/2} core level was measured as a reference. Depth

profiles of the samples were obtained by measuring the core level peaks for the elemental species (Ga3d, Ga3p P2p, N1s) and native surface oxides (O1s and C1s).

Energies were specifically chosen to avoid Auger peaks. Measurements were taken at photon energies adjusted according to the binding energies of a given species (Eqn. 2.1) to give emitted electrons kinetic energies of 200, 450, 750 and 900 eV. These measurements equate to escape depths (assuming grazing incidence angle) of 9, 14.85, 21.25, and 24.3 Å respectively [9].

3. RESULTS

XPS Measurements

XPS results are distinguishable based upon two variables: nitrogen content and corrosion treatment of the samples. A number of features are present and worthy of note, but a limited selection will be presented here.

In all cases, there were a number of oxides present on the samples, generally seen at binding energies higher than the pure species. The Ga3d spectrum is shown as an example, with the oxides denoted (Figure 3.1). The intensity of these oxides relative to the species measured decreases at higher energies.

The Ga3d spectra at all energies show a decrease in gallium content near the surface after corrosion (Figure 3.2).

At all energies, the uncorroded nitrogen spectra for the $\text{GaP}_{1-x}\text{N}_x$ ($x = 0.02$) sample shows two peaks, one corresponding to N bonded to Ga in the bulk, the other to NO_x and NH_x on the surface. The bulk peak is higher in binding energy by approximately 2.5 eV (Figure 3.3), while the second, smaller peak does not appear in the corroded sample spectra. These features are also visible in the $\text{GaP}_{1-x}\text{N}_x$ ($x = 0.002$) samples.

4. DISCUSSION AND CONCLUSIONS

Qualitatively, the samples showed agreement with previous literature: the addition of nitrogen improves the ability of the GaP to produce hydrogen. The XPS data supports this by showing consistent differences between nitrogen containing samples and the GaP.

The large oxide peak shows evidence of oxides observed in a previous study of GaAs, which, as another III-V compound, behaves similarly to GaP. C.C. Surdu-Bob *et al.* report the binding energy of Ga₂O₃ at 20.7 eV ± 0.1 eV, Ga₂O at 20.1 and Ga(OH)₃ at 21.6 eV. [10] Thus, the gallium oxides (denoted on Figure 3.1) were most likely in the forms Ga₂O, Ga₂O₃ and Ga(OH)₃. The oxide on phosphorus appeared in a peak centered at a binding energy of approximately 133 eV, which matches P₂O₅ (binding energy of approximately 133.6 eV).

The gallium-poor surface after corrosion is significant in determining the corrosion mechanism. A proposed corrosion mechanism in agreement with the Ga depletion is:



The depletion of surface Ga matches with both mechanisms. However, the corrosion solutions are being submitted for inductively coupled plasma mass spectroscopy (ICP-MS) analysis to identify the species present.

The disappearance of the second nitrogen peak in GaPN samples (Figure 3.3) indicates the migration of nitrogen from the bulk toward the sample surface as a result of corrosion. Based upon binding energies, the smaller peak at lower binding energy indicates nitrogen added to the sample during MOCVD, or “bulk” nitrogen. The larger peak represents nitrogen oxidized by exposure to air while mounting them on the sample holder. Since the bulk peak is not apparent in the corroded spectra taken at the same photon energy, the conclusion is that the bulk nitrogen

migrated to the sample surfaces during corrosion. One possible explanation for the surface nitrogen is the formation of GaN (band gap of approximately 3.2) during corrosion. Since GaN has a larger band gap, it has a tendency to be more resistant to corrosion. In this case, the semiconductor would actually be behaving like a tandem cell: the smaller band gap of GaP for maximum solar absorbance, but the larger band gap adding stability. The GaN may be undetectable currently, as the sample oxidized after removal from the electrolyte. But, as there are a number of electronic consequences of nitrogen implantation, investigations are currently underway to make final conclusions as to the significance of the nitrogen migration.

In future analysis, ICP-MS analysis will detect the presence of any species desorbed from the surface of the $\text{GaP}_{1-x}\text{N}_x$ during corrosion. These may have been produced either directly from the semiconductor reactions, or as a result of interaction with the acidic solution. The results of these tests should indicate what species form during corrosion. The samples have also been submitted to view topography with a SEM or TEM. Hopefully, analysis of the semiconductor surface combined with knowledge of the solution composition will yield a complete set of corrosion products from which the reaction mechanisms can be deduced. By learning about the surface, it may be possible to eventually engineer the surface of the semiconductors to increase the lifetime of a hydrogen producing PEC.

5. ACKNOWLEDGEMENTS

This research was conducted at the Stanford Synchrotron Radiation Laboratory. Thanks first to Theanne Schiros for her undying enthusiasm for the project and the time she spent teaching me this summer. Thank you to Jen Leisch, whose constant flux of wisdom kept the project moving. I would also like to thank Theanne and Jen for a constant flow of food, and Trader Joe's for

producing said food. I gratefully acknowledge the many hours that Lars-Åke Näslund spent at the beamline with us instead of sleeping, the patience and dedication of Anton Nikiton, the pearls of wisdom provided by Hirohito Ogasawara, the general helpfulness of Mike Toney and the constant assistance from Experimental Support. Thank you also to everyone who even so much as answered one of my numerous questions or caused me to smile. Finally, we thank Anders Nilsson for his guidance and his efforts to introduce such renewable energy projects at the Stanford Linear Accelerator Center.

6. REFERENCES

- [1] *Energy Information Administration*, 2004, <http://www.eia.doe.gov/>.
- [2] T. Bak *et al.*, “Photoelectrochemical hydrogen generation from water using solar energy. Materials Related Aspects,” *International Journal of Hydrogen Energy*, vol. 27, pp 991 – 1022, 2002.
- [3] J. Leisch. *CuInSe₂ and Related Alloy Thin Film Semiconductors for Photoelectrochemical Hydrogen Production*, PhD Thesis, Golden, Colorado, 2006.
- [4] H. Gerischer, “On the stability of semiconductor Electrodes against photodecomposition,” *Journal of Electroanalytical Chemistry*, vol. 82, pp133-143, 1977.
- [5] T. Deutsch. *Sunlight, Water and III-V Nitrides for Fueling the Future*, PhD Thesis, Boulder, Colorado, 2006.
- [6] W. D. Callister. *Materials Science and Engineering: An Introduction, Fourth Edition*, New York: John Wiley and Sons, pp 603, 1997.

- [7] N. Martensson and A. Nilsson, "High-Resolution Core-Level Photoelectron Spectroscopy of Surfaces and Adsorbates," in *Applications of Synchrotron Radiation*, W. Eberhardt, Ed. Berlin: Springer-Verlag, pp. 65-125, 1995.
- [8] P. Pianetta, "Low-energy electron ranges in matter," in *Center for X-ray Optics and Advanced Light Source: X-ray Data Booklet*, Berkeley: Lawrence Berkley National Laboratory, p 3-11, 2001.
- [9] S. Tanuma *et al.*, "Calculations of Electron Inelastic Mean Free Paths: III. Data for 15 Inorganic Compounds over the 50-2000 eV Range," *Surface and Interface Analysis*, vol 17, pp. 927, 1991.
- [10] C.C. Surdu-Bob *et al.*, "An X-Ray photoelectron spectroscopy study of the oxides of GaAs," *Applied Surface Science*, vol. 183, pp 126-136, 2001.

7. FIGURES

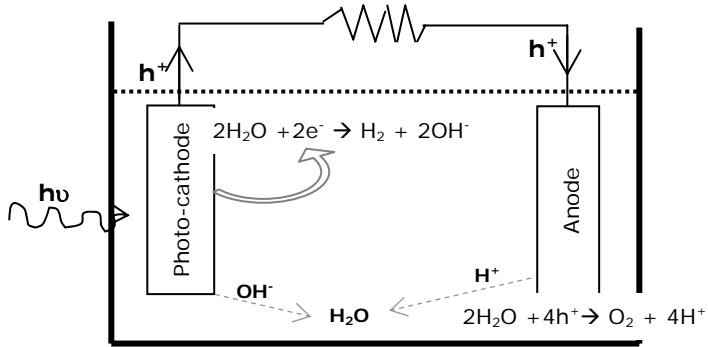


Figure 1.1. Photo-electrochemical cell arrangement for electrolysis

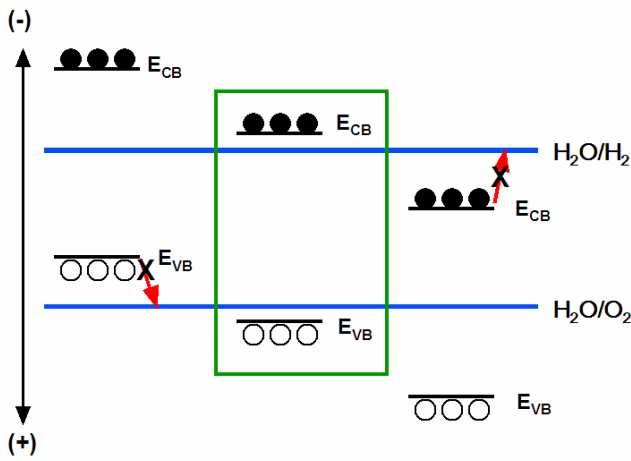


Figure 1.2. Band edge position requirements for a PEC semiconductor material. The conduction band (E_{CB}) and valence band (E_{VB}) energies must straddle the water redox potentials. Figure from Leisch [3].

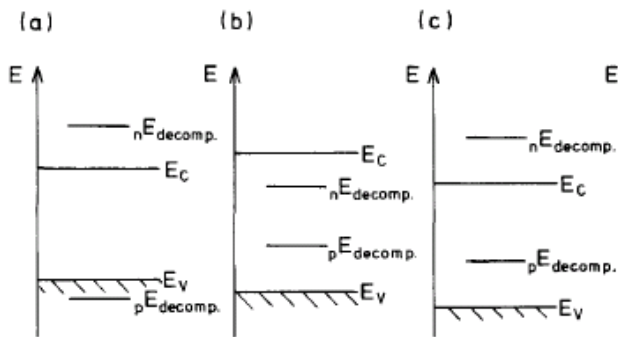


Figure 1.3. Typical correlations between energy positions of band edges and decomposition potentials, controlling stability against photodecomposition. (a) Stable, (b) unstable, (c) stable against cathodic decomposition. Figure from Gerischer [4].



Figure 2.1. NREL electrochemical cell made of Pyrex and Teflon. Semiconductor directly behind light, Pt counter and Ag/AgCl reference electrodes used.

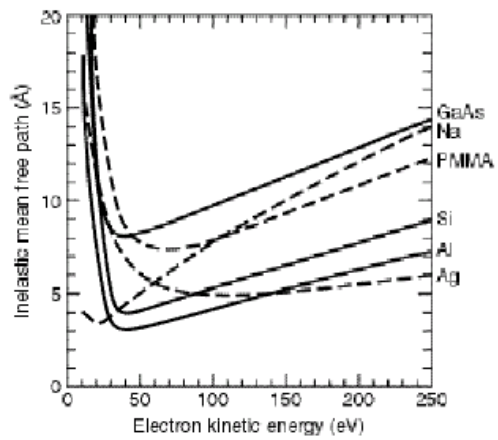


Figure 2.2. Inelastic mean free path as a function of core electron kinetic shown for six different materials. [9]

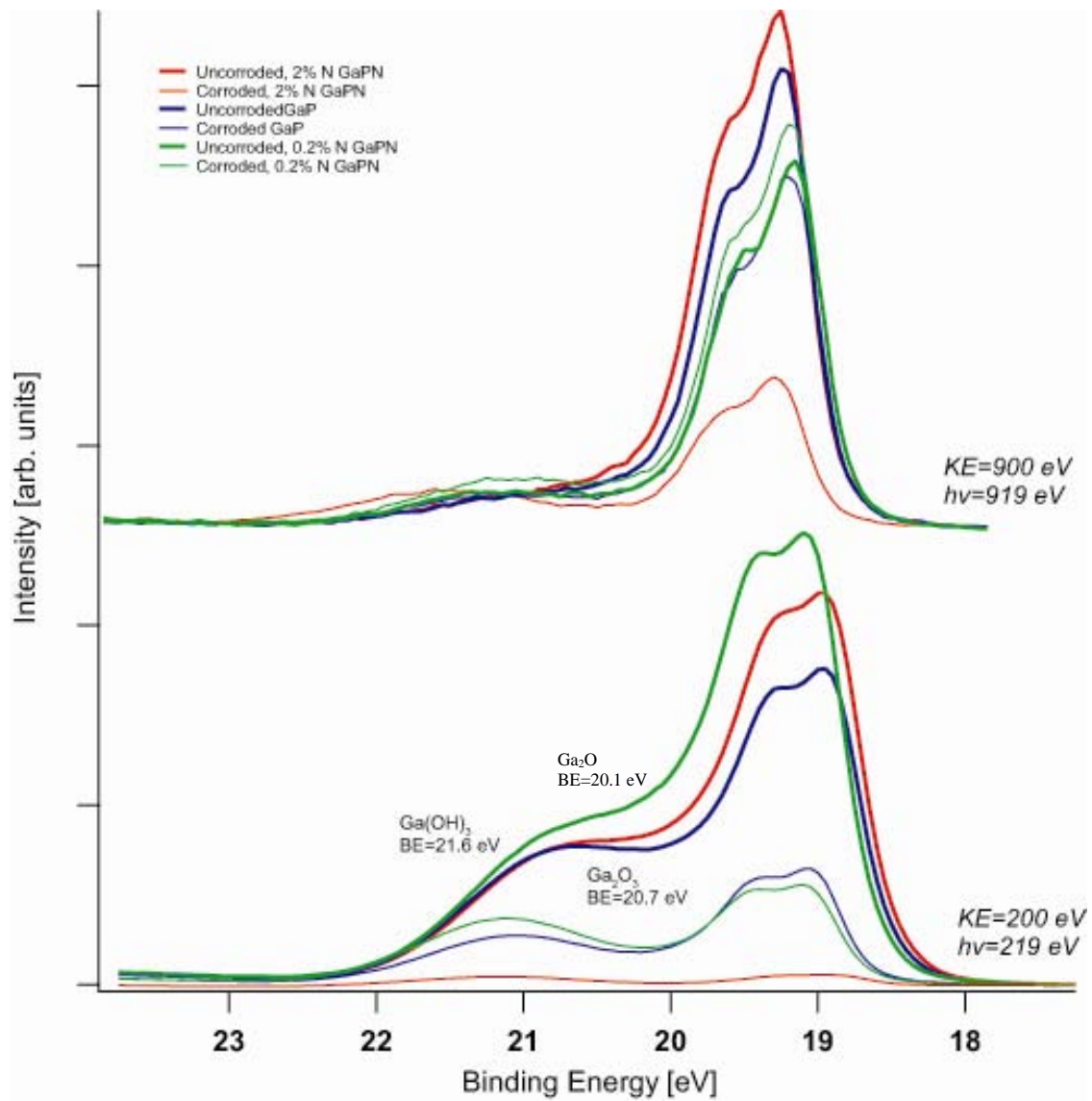


Figure 3.1. Ga3d spectra at photon energies of 219 eV and 919 eV. Suspected oxides are labeled on the lower energy spectrum. The intensities of the oxides is much weaker at higher energies.

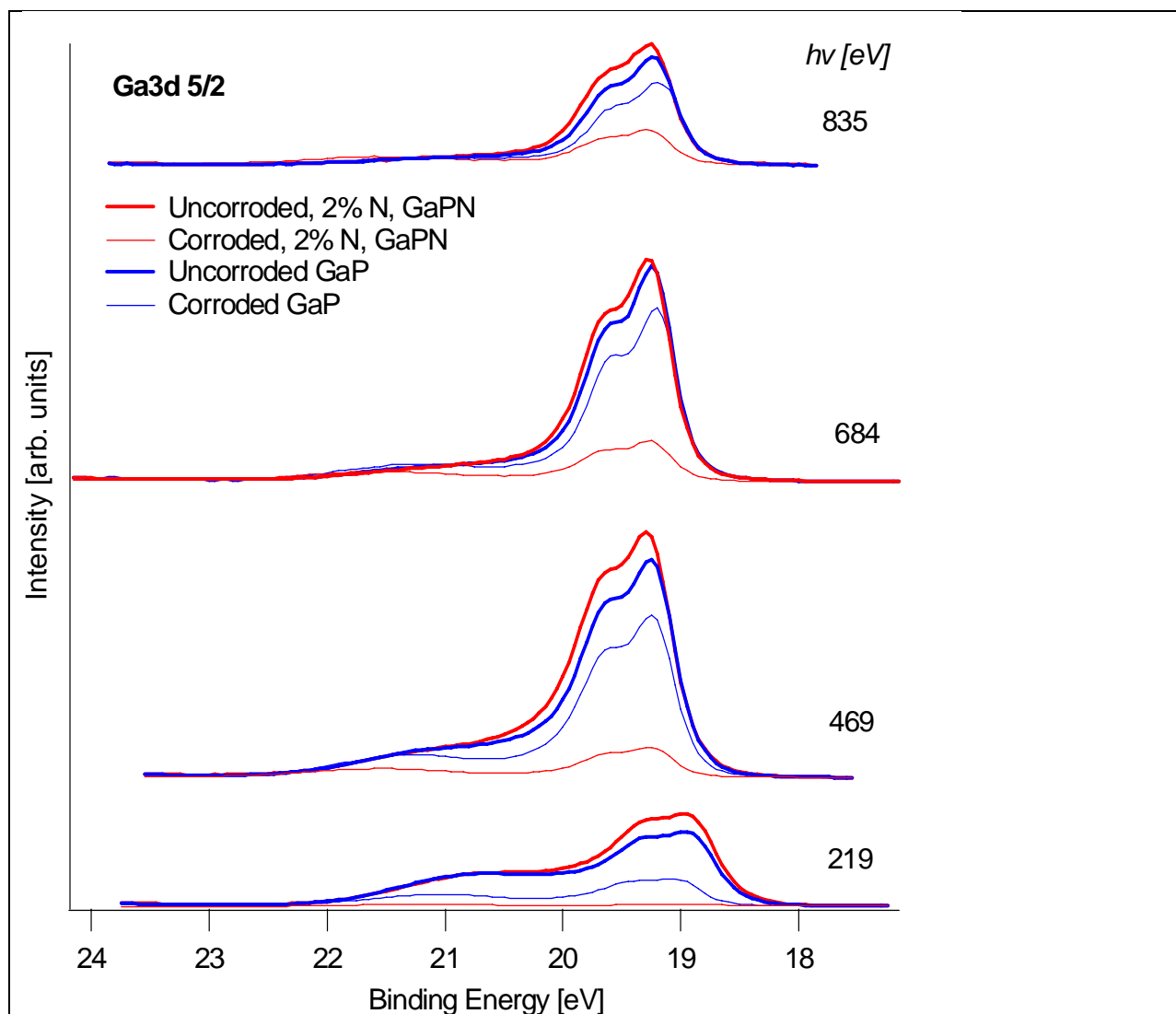


Figure 3.2. Ga3d spectra at all four tested photon energies of 219 eV and 919 eV. Corroded samples (thin lines) show less intensity than their respective uncorroded samples, regardless of nitrogen content. The 0.02% nitrogen sample behaved similarly.

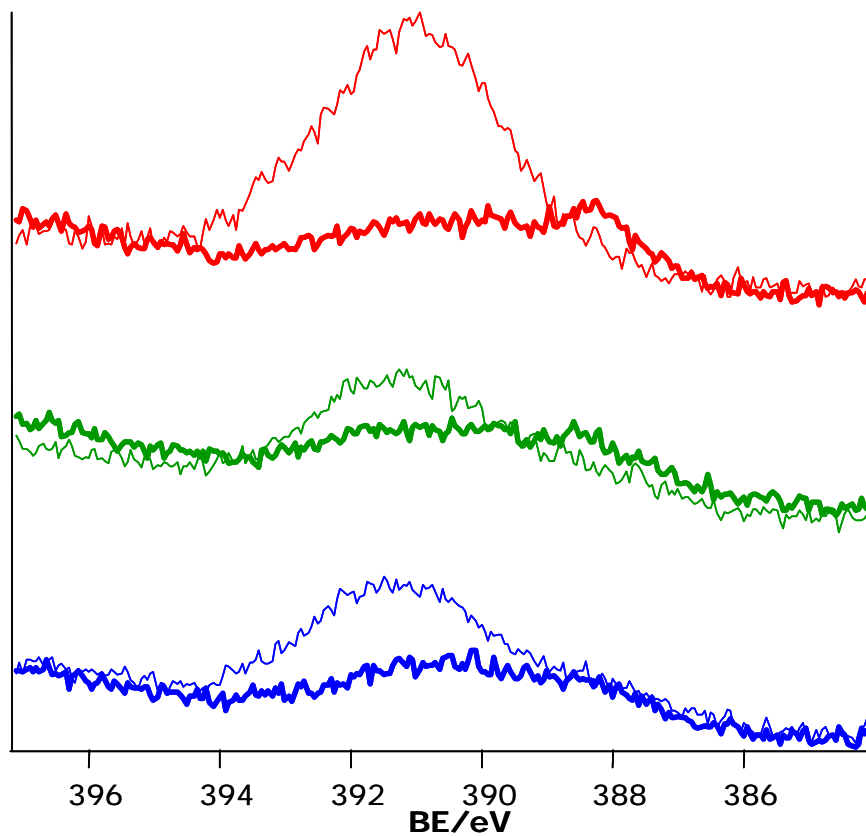


Figure 3.3. N1s spectra for GaP and GaPN_{0.02} as a function of intensity. Bulk nitrogen (maximum at 397 eV) is apparent in the uncorroded sample, but not in the sample after corrosion. The GaP samples only show nitrogen surface contamination (maximum at 400 eV), before and after corrosion.